We are IntechOpen,
the world's leading publisher of
Open Access books
Built by scientists, for scientists

6,900
Open access books available

186,000
International authors and editors

200M
Downloads

Our authors are among the

154
Countries delivered to

TOP 1%
most cited scientists

12.2%
Contributors from top 500 universities

CLARIVATE ANALYTICS
BOOK CITATION INDEX
INDEXED

WEB OF SCIENCE™

Selection of our books indexed in the Book Citation Index
in Web of Science™ Core Collection (BKCI)

Interested in publishing with us?
Contact book.department@intechopen.com

Numbers displayed above are based on latest data collected.
For more information visit www.intechopen.com

PIV Measurements on Oxy-Fuel Burners

Boushaki Toufik[1] and Sautet Jean-Charles[2]
[1]ICARE-CNRS, Avenue de la Recherche Scientifique, Orléans, University of Orléans,
[2]CORIA, CNRS-Université et INSA de Rouen, Saint Etienne du Rouvray
France

1. Introduction

This chapter concerns the application of the PIV measurements in a semi-industrial combustion system. The emphasis is on oxy-fuel burners with multi-jets. The mixing and the dynamic field for both reacting and non-reacting flows are investigated.

Nowadays, combustion occupies a prominent place to meet the increasing needs of our economic world, in fields as diverse as: the production of electrical energy; the space heating, the development of building materials, the metallurgy; the land and air transport; the synthesis of many chemicals in flames; the production of hydrocarbons from crude oil in refineries, etc. Mastering combustion obtained under as varied conditions requires: a knowledge of more advanced fundamental phenomena governing the reaction processes; a " know-how" to an optimal implementation in terms of energy (efficiency) and in terms of pollution (air pollution, noise).

The evolution of pollution standards and the optimization of combustion chamber performances require a development of new burner types and the improvement of combustion techniques. The industrialists are turning to a new burner generation with separate injection of fuel and oxidant. Design of these burners requires the knowledge of mechanisms controlling the stabilization of flame and the production of pollutants. The present study concerns the control of turbulent natural gas-oxygen flames resulting from burners with aligned separated jets. One possibility to understand the structure and mechanism of flame stabilization more accurately is to analyze the structure of the flow by means of particle image velocimetry (PIV) (Raffel and al., 1999). This method allows direct velocity measurements without and with combustion. The application of PIV in industrial scale flame has been already demonstrated on a 1MW experimental boiler (Honoré et al., 2001).

Oxy-fuel combustion, air is substituted by pure oxygen, is characterized by a higher adiabatic flame temperature, a higher flame velocity, a lower ignition temperature, and a wider flammability range that is the case of combustion with air (Baukal and Gebhart, 1997; GEFGN, 1983; Perthuis, 1983; Ivernal and Marque, 1975). This oxy-fuel combustion allows to have a better thermal efficiency and a better stabilization of flame. Oxy-fuel burners have been adopted in a wide range of industrial furnaces to improve productivity and fuel efficiency, to reduce emissions of pollutants, and, in some applications, to improve product quality and yield or to eliminate the capital and maintenance costs of air preheaters

(Baukhal, 2003). Furthermore, the use of oxy-fuel combustion in separated-jet burners open interesting possibilities in the NOx reduction, and the modularity of flame properties such as stabilization, topology and flame length (Sautet et al., 2006, Boushaki et al., 2007).

Flames from burner with multiple jets have many practical situations. Several studies have been published on the structure and development of non-reacting multiple jets (Krothapalli et al., 1980; Raghunatan et al., 1980; Pani and Dash, 1983; Simonich 1986; Yimer et al., 1996; Moawad et al., 2001). However, the studies of multiple jet flames are mostly limited, for example, flame developing in still air without confinement (Leite et al., 1996) or in a wind tunnel with cross flow (Menon and Gollahali, 1998). Lee et al. (2004) studied the blowout limit considering the interaction of multiple non premixed jet flames and giving a number of variables such as distance between the jets, the number of jets and their arrangements. Lenze et al. (1975) have studied the mutual influence of three and five jet diffusion flame, with town gas and natural gas burners. Their measurements concern concentrations, flame length, and flame width in free and confined multiple flames. The burner configuration used in this work is composed of three round jets, one central jet of natural gas and two lateral jets of pure oxygen.

For the separated jet burner, the principle is based on the geometrical separation of its nozzles. The separation of jets allows high dilution of reactants by combustion products in the combustion chamber. This dilution leads to a lower flame temperature and homogenization of temperature throughout the volume of the flame, and consequently a decline in NOx production. However, the configuration of separated jets, which contributes to the dilution of reactants, may become unfavorable to the stabilization of flame. Indeed, this dilution may be controlled by various burner parameters, such as exit velocities of reactants and the distance between the jets. In previous papers of the authors (Boushaki et al., 2007), the characteristics of flames in burners with separated jets have been studied versus the burner parameters such as exit velocities, separation distance between jets and angle of injection. It is interesting to note that the inclination of jets allows to improve the flame stability and above all reduces significantly the NOx (Boushaki et al. 2008). The present chapter focuses on the dynamic behavior of three jet interactions in more detail by varying angle of the side oxygen jets.

Controlling the flows has been the focus of numerous investigations. The objectives of flow control (passive and active) differ according to the considered industrial application. Among these aims are the improvement of mixing with ambient air (Davis, 1982 ; Denis et al., 1999), the limitation of combustion instabilities (Lang et al., 1987; Candel, 1992), the enhancement of heat transfer of flame (Candel, 1992), the decrease of pollutant emissions (Delabroy, 1998; Demayo, 2002) and the reduction of noise engendered in some combustion chambers (Barrère and Williams, 1968; Strahle, 1978). The two dominant methods of passive flow control include noncircular nozzles (e.g., Ho and Gutmark, 1987; Gutmark and Grinstein, 1999, Gollahalli et al., 1992) or the use of tabs at the nozzle exit (e.g., Bradbury and Khadem, 1975; Ahuja, 1993; Hileman et al., 2003). The active control consists in injecting external energy through actuators .The quality of the control depends directly on the design of the actuators. Some of them are specific to combustion applications but most actuation techniques are encountered in both reactive and non-reactive applications, such as loudspeakers (Bloxsidge et al., 1987, McManus et al., 1993), small jet actuators (Lardeau et al., 2002 ; Faivre and Poinsot, 2004, Boushaki et al., 2009), synthetic jets (Davis, A. Glezer

1999; Tamburello and Amitay, 2008) and flaps (Susuki et al., 1999). It has been proven in the literature that jet actuators have drastic effects on mixing and flow dynamics. In fact, jets actuators are capable to change the flow structure, to act on mixing between the reactants, and thus on the flame characteristics such as stability and flame size, as well as pollutant production. The perpendicular arrangement of tube actuators at the periphery of a main jet can confer to the flow a helical movement (swirl). This kind of swirl with actuators has very significant effects on the flow. Ibrahim et al. (2002) and Faivre and Poinsot (2004) indicated that a radial fluid injection into the main jet enhances mixing with the surrounding air. Béer and Chigier (1972), and Feikema et al. (1990) showed that the addition of swirl significantly changes the aerodynamic pattern and can be used to stabilize the flame. The helical fluid flow creates a recirculation zone, allowing dilution with combustion products, and the decrease of the flame temperature limiting the NOx production (Syred and Béer, 1974; Schmittel et al., 2000; Coghe et al., 2004).

The present chapter reports the results of an experimental investigation of the dynamic field on a burner with 25 kW power composed of 3 jets, one central jet of natural gas and two side jets of pure oxygen. The velocity measurements were carried out using Particle Image Velocimetry (PIV) in both cases of non-reacting flow and reacting flow inside the combustion chamber. Two control systems, one passive and one active, are developed and added to the basic burner to improve the combustion process and to ensure the stabilization of flame and pollutant reductions. The passive control is based on the slope of side oxygen jets towards the central natural gas jet in a triple jet configuration. The active control concerns the use of four small jet actuators, placed tangentially to the exit of the main jets to generate a swirling flow. These actuators are able to strongly modify the flow structure and to act on mixing between the reactants and consequently on the flame behavior.

Nomenclature			
d	tube internal diameter, mm	*Greek symbols*	
M	initial velocity ratio ($M = (U_{ng}^0 / U_{ox}^0)$)	θ	oxygen jet angle, (°)
$\dot{m}$	mass flow rate, kg.s^{-1}	μ	dynamic viscosity, g.m.s^{-1}
r	ratio of volumetric flow rate ($r = \dot{m}_{act} / m_{tot}$)	ρ	gas density, kg.m^{-3}
Re	Reynolds number ($= \rho U^0 d / \mu$)		
S	separation distance between the jets, mm	Subscripts	
SW2J	Burner configuration with 2 jets	ac	actuator
SW3J	Burner configuration with 3 jets	jet	main jet
U^0	nozzle exit velocity, m.s^{-1}	cl	centerline
U	longitudinal mean velocity, m.s^{-1}	lo	lift-off
u′	longitudinal velocity fluctuation ms^{-1}	ng	natural gas jet
V	radial mean velocity, m.s^{-1}	ox	oxygen jet
v′	radial velocity fluctuation, m.s^{-1}	tot	total
x, z	radial and longitudinal coordinate, mm		

2. Burner and operating conditions

2.1 Basic configuration of the burner

The basic configuration of the burner consists of three round tubes, one central of natural gas and two laterals of pure oxygen. A schematic of the oxy-fuel burner apparatus is shown in Fig. 1. This burner can operate with only two jets if the entire oxygen flow rate is injected into a single tube. Fuel and oxidizer flow rates are constant for all experiments to ensure constant power flames of 25 kW ($\dot{m}_{ng} = 556 \times 10^{-3} kg.s^{-1}$, $\dot{m}_{Ox} = 1964 \times 10^{-3} kg.s^{-1}$). The natural gas ($\rho_{ng} = 0.83$ kg.m^{-3}) flows from the central tube (diameter d_{NG}=6 mm, length 250 mm) and pure oxygen ($\rho_{ox} = 1.35$ kg. m^{-3}) flows from the two side jets (diameter d_{Ox}=6 mm or 8 mm, length 250 mm). The natural gas composition is: 85% CH_4; 9% C_2H_6; 3% C_3H_8; 2%N_2; 1% CO_2; plus traces of higher hydrocarbon species. The flow rate of natural gas is controlled by a regulator of mass flow rate TYLAN RDM 280; the oxygen is regulated by sonic throats calibrated by a classical flowmeter in function of pressure.
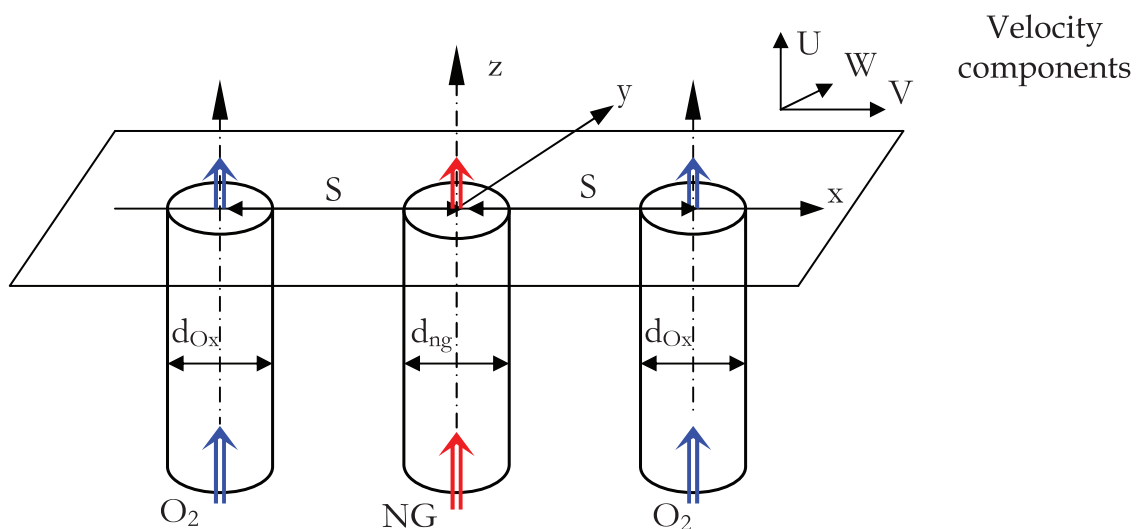
Fig. 1. Schematic diagram of oxy-fuel burner

In the case of reacting flow, the oxy-fuel flames takes place inside a combustion chamber of 1 m-high with square cross section of 60×60 cm. The lateral walls are refractory lined inside and water cooled outside of the combustion chamber. Optical access is provided by quartz windows at many vertical positions of the combustion chamber. The burner is located at the centre of the bottom wall of the combustion chamber (more details, see Boushaki et al. 2009).

2.2 Passive control system

The control technique consists in inclining the side oxygen jets towards the natural gas jet as shown in Fig. 2. The angle of oxygen jets (θ) compared to the vertical direction varies from 0° to 30° (0, 10, 20, 30°). The internal diameters of natural gas and oxygen tubes (d_{ng} and d_{ox}) are both 6 mm. Exit velocities for the natural gas and the oxygen jets without control (θ=0°) inferred from the flow rates are respectively are $U_{NG}^0 = 23.7$ m/s and $U_{Ox}^0 = 25.7$ m/s. The separation distance between the jets (S) is fixed at 12 mm. The exit Reynolds numbers of the natural gas jet and the oxygen jet are Re_{ng}= 10772 and Re_{ox}= 10936 respectively.
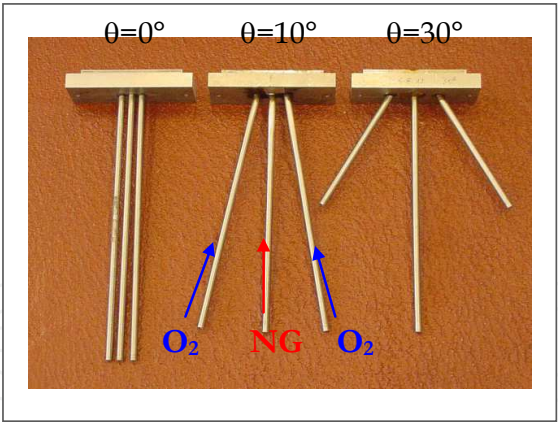
Fig. 2. Photo of burners with angle injection 0°, 10° and 30°

2.3 Active control system

The active control is applied using four small jet actuators arranged slightly upstream the exit of the main jets. Fig. 3 shows the oxy-fuel burner fitted with actuators. Each nozzle is equipped with four small control jets placed tangentially around the main jets. This kind of tangential control generates a swirling motion in the flow, its intensity being controlled by the flow rate in the actuators. The exit diameter of the jet actuators (d_{act}) is 1 mm and their position relative to the main jet exit is z = -1mm. In the present work, the rotating flow intensity is quantified by the ratio of volumetric flow rates of actuators ($\dot{m}_{act}$) and total ($\dot{m}_{tot}$), which varies from 0 to 30%; it is given by:

$$r = \frac{\dot{m}_{act}}{\dot{m}_{tot}} \tag{1}$$

where $\dot{m}_{tot} = \dot{m}_{jet} + \dot{m}_{act}$ and $\dot{m}_{jet}$ is the flow rate of the main jet ($\dot{m}_{tot} = \dot{m}_{NG}$ for the fuel flow rate and $\dot{m}_{tot} = \dot{m}_{Ox}$ for the oxygen flow rate). The subscripts "tot" and "act" are valuable for both reactants (oxygen and natural gas). For the present configurations, the swirl number (S_n) characterizing rotating flows is an increasing function of the flow rate ratio (r).
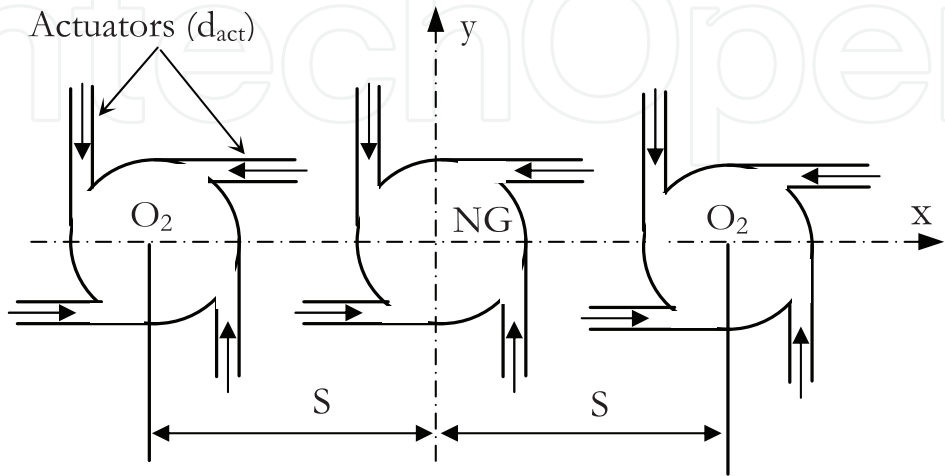

Fig. 3. Schematic view of main nozzles with tangential tube actuators

The swirl number is a dimensionless quantity defined as (Beèr and Chigier, 1972; Sheen et al. 1996):

$$S_n = \frac{G_\varphi}{R G_x'} \tag{2}$$

where G_φ is the axial flux of the tangential momentum, G_x' is the axial flux of axial momentum, and R is the exit radius of the burner nozzle.

$$G_\varphi = \int_0^R (Wr)\rho U\, 2\pi r\, dr \tag{3}$$

$$G_x = \int_0^R U\rho U\, 2\pi r\, dr \tag{4}$$

U and W are the longitudinal and tangential components of the velocity respectively.

The corresponding geometrical swirl number, defined following the previous work (Boushaki et al. 2009) as:

$$S_n = \frac{\frac{\dot{m}_{act}}{\dot{m}_{jet}}}{1 + \frac{\dot{m}_{act}}{\dot{m}_{jet}}} \left[\frac{2\left(d_{act}^2 + 3R(R - d_{act})\right)}{3R(2R - d_{act})} \right] \tag{5}$$

is calculated from the flow rate of main and actuator jets ($\dot{m}_{jet}$ and $\dot{m}_{act}$), the radius of the main jet and the jet actuators (R and d_{act}). From r=0 to 30%, the swirl number varies from 0 to 0.25 for R=3 mm and to 0.26 for R=4 mm.

The exit parameters of the two studied configurations are listed in Table 1. $U°$, Re and M are the jet exit velocity, Reynolds number and initial velocity ratio (U_{NG}^0 / U_{Ox}^0) respectively. In the presence of jet actuators, the exit velocity of the main jet decreases when the flow rate ratio (r) increases since a portion of the total flow rate is injected into the tube actuators. Conversely, the exit velocity of jet actuators increases with r.

Burner configuration	Number of Jet	S (mm)	Gas	d (mm)	U^0 (m/s)	Re	M= U_{NG}^0 / U_{Ox}^0
SW3J	3	20	Natural gas	d_{ng}=6	23.7	10772	1.64
	1 NG, 2 O$_2$		Oxygen	d_{ox}=8	14.45	8198	
SW2J	2	20	Natural gas	d_{ng}=6	23.7	10772	0.82
	1 NG, 1 O$_2$		Oxygen	d_{ox}=8	28.91	16400	

Table 1. Burner configurations and parameters. The notation SW3J means Swirl with three main jets (1NG and 2O$_2$)

3. PIV system: Experimental set-up and procedure

Particle Image Velocimetry (PIV) is a laser diagnostic method which has been developed in parallel with Laser Sheet Visualization (LSV)). As with LSV, The PIV is based on the collection of images of Mie scattering of fine particles seeded in the flow. Processing of these particle images provides instantaneous data on two velocity components in a plane crossing the flow. Then, the mean and root-mean-square (rms) velocity fields can be easily deduced from statistical studies of the instantaneous measurements sequences.

Fig. 4 shows a schematic diagram of the PIV system. It includes a laser sheet that illuminates the zone of flow studied, a CCD camera, a PC for data acquisition and a control unit for synchronization. The laser used is double-pulsed Nd-YAG (Big Sky CFR200 Quantel) with a wavelength of 532 nm and a frequency of 10 Hz. Laser energy is adjustable and can be increased up to 150 mJ per pulse with pulse duration of 8 ns. The laser sheet is formed by a first divergent cylinder lens, which spreads out the beam then by second convergent spherical lens, which focuses the sheet. The signal of Mie scattering emitted by particles is collected perpendicularly by a CCD camera FlowMaster of Lavision (12-bit dynamic and 1280×1024 pixels resolution) with a 50 mm lens F/1.2 Nikkon. In reacting flow measurements, to reject the bright luminosity from the oxy-flame, an interference filter (532 nm centre, 3 nm bandwidth) was placed in front of the imaging lens. The time delay between the laser pulses varies from 8 to 20 μs according to the case. For each operation condition, up to 400 pairs of instantaneous images were collected.
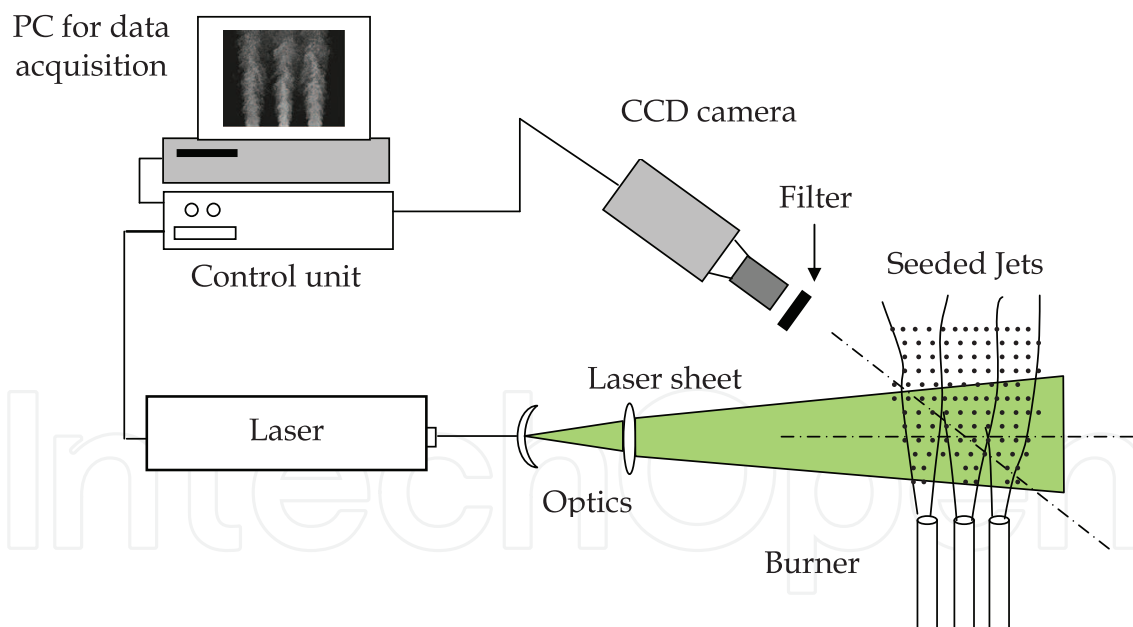

Fig. 4. Schematic view of a PIV system. The CCD camera and the laser sheet are perpendicular

For the non-reacting flow, the jets are seeded with olive oil particles (~ 3 to 4 μm in diameter) whereas for reacting flow they are seeded with zirconium oxide (ZrO_2) particles (~ 5 μm diameter). The reasons for the choice of these ZrO_2 particles are: a high resistance of high temperatures generated by the oxy-combustion (melting point 2715°C), a good refractive index (2.2) which allows a good light scattering, and a little size for a better mixing

in the flow. Fig.5 illustrates the two systems of seeding particles. For olive oil particles, the seeding system is an atomizer based on Venturi principle to produce fine particles. For ZrO_2 particles, the system consists of tubes equipped with porous plates, placed at the level of exit gases. The gas passes through the porous medium and drags a certain quantity of particles providing a uniform seeding. Concentration of particles is controlled by valves through the gas flow rate in the line of seeding. A particular attention has been carried in the drying of particles before their injection in the seeding system in order to limit agglomerates. The measurements were conducted with seeding rates relatively low to avoid perturbing the flow. Particles in fact can modify the characteristics of the flow if they are introduced in high quantity, and can even blow out the flame. The criterion assuring a good track of flow by particles is respected here, since the Stokes number, defined as the ratio between the response time of particles and a time characteristic of the flow, obtained in the present experiments is much lower than unity (St <<1). For example, $t_p \approx 0.015$ms in the case of oxygen and oxide zirconium particles ($t_p = 2\rho_p r_p^2 / 9\mu_{CH4}$: $\rho_p = 5600\,kg.m^{-3}$, $r_p = 0.5\,\mu m$, $\mu_{CH4} = 20,18.10^{-6}\,Pa.s$), with the frequency of 1000Hz, the Stokes number is about 0.015.
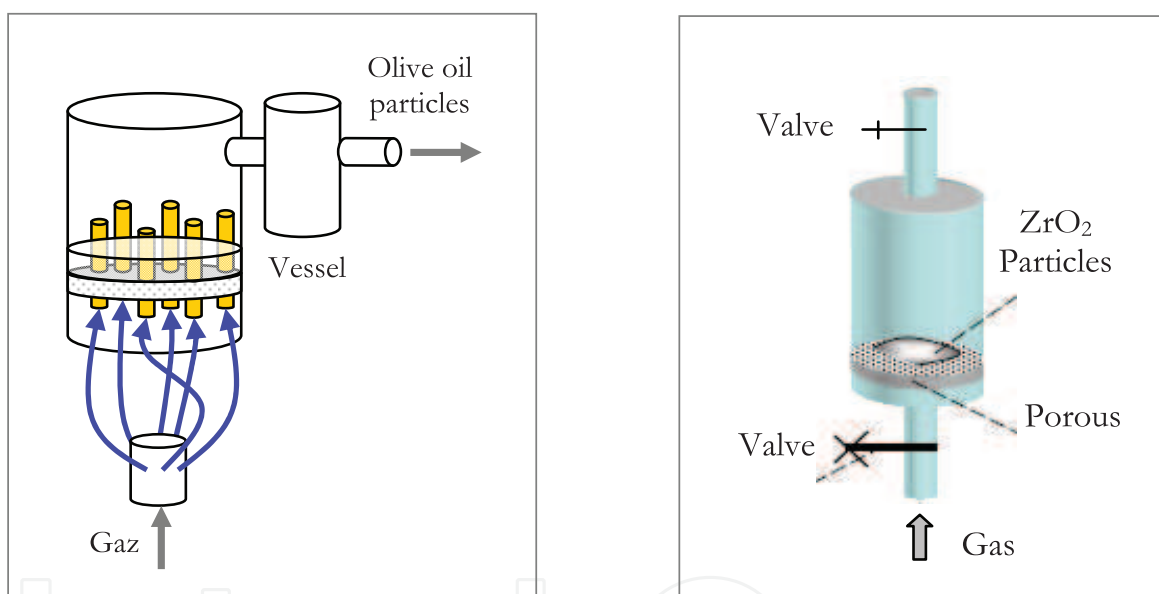

Fig. 5. Seeding systems, for olive oil particles in non-reacting flow (left), for ZrO2 particles in reacting flow (right)

The Davis Lavision software package uses a cross-correlation technique to find the average particle displacement in each subregion (32×32 pixels) of the image. The velocity is found by dividing the particle displacement by the time between laser pulses. The sub-pixel displacement was estimated by means of Gaussian peak of fitting (Lecordier and Trinité, 2003). With a maximum displacement of 8 pixels, this would correspond to less than 2% uncertainty in final velocity measurement. It was necessary to carry out a post processing to detect and correct the aberrant vectors which appear after cross-correlation calculations. Detection of false vectors can be done by the size of the vector. In this case, it is necessary to locate all vectors above a certain threshold of velocity according to the expected results. The direction of vectors can also help to identify false vectors knowing a priori the direction of flow. For that the *allowable vector range*, restricting the filtered vectors to a user specified in

units of pixel was performed. A range may be specified for each component of velocity U and V (range of ± value). Any vectors outside this range are removed. In some cases, in particular for instantaneous images, filters to refine the results are used as local median filter or regional median filter based on the neighbouring vectors.

4. PIV measurements on burners with inclined jets

4.1 Instantaneous and mean velocity fields

For the inclined injectors (see Fig. 2), the shape of exit nozzles is elliptical rather than round. Therefore, the profile of velocity for inclined jet at the exit nozzle is quite different to the one of a straight jet. That is why results of the exit velocities are provided; they are very useful for numerical studies. Fig. 6 shows the profiles of mean velocities near the burner exit (z=3 mm) in the non-reacting flow. For the side jets, the longitudinal mean velocity, U, decreases with the angle of the oxygen jets, however, the radial velocity, V, increases as a result of the deflection of injectors. It is noted that from the velocity profiles of PIV measurements, the flow rates at the exit nozzles are calculated and are in very good agreement with the flow rate injected.
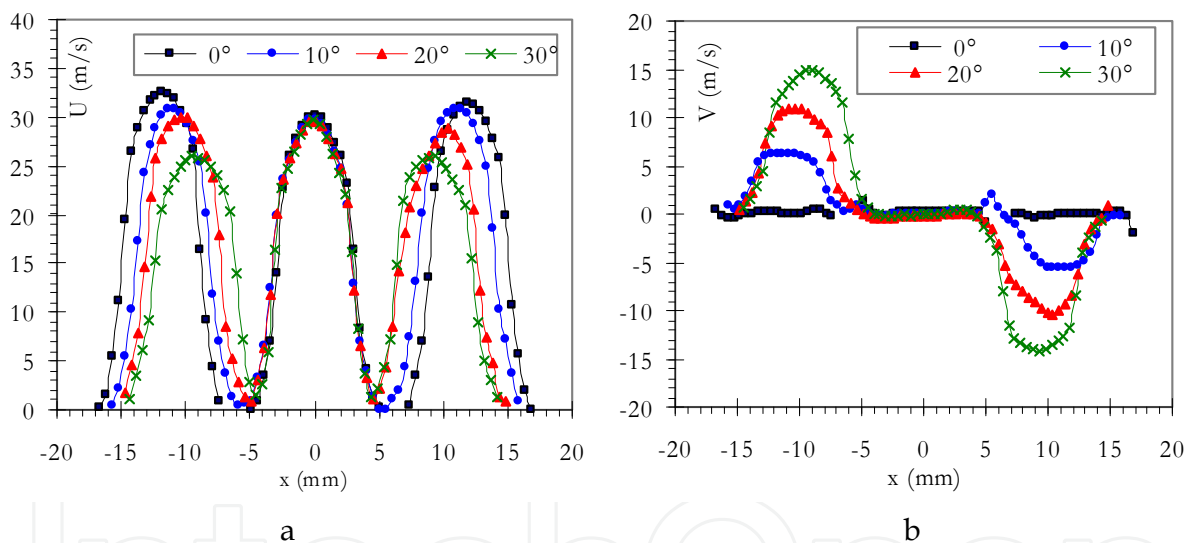
Fig. 6. Radial profiles of longitudinal (a) and radial (b) velocities at exit nozzles (z=3mm) in non-reacting flow for the oxygen jet angle, θ = 0°, 10°, 20° and 30°

Fig. 7 shows an example of instantaneous velocity fields, taken among 400 instantaneous fields, for oxygen jet angles 0° and 30°, with the longitudinal velocity U (along the vertical direction) in color scale. The burner configuration is highly three-dimensional, since some discontinuous aspects of streamlines are observed on the instantaneous velocity fields. However, this aspect is not visible in Fig. 8 because the images averaging remove the discontinuities and high gradients on the velocity distribution. For the central jet, the longitudinal velocity varies weakly and the radial velocity is nearly zero in the near nozzle field. More downstream, the side jets affect the central jet and its radial velocity is no longer zero. In the far field, vortices appeared in the region of the mixing layer between the jet and the ambient air (for θ=30). At the merging zone of three the jets, gradients in the velocity

values are noted characterizing the three-dimensionality, particularly when the side jets are inclined. This is due to the transverse flow of jets and the elliptical shape of inclined nozzles, as it was shown in the paper of Gutmark and Grinstein (1999) where the entrainment rate and the mixing for elliptic jets are more significant compared to the round jets. Mean velocity fields, obtained by averaging 400 instantaneous images, in non-reacting flow for the jet angles 0° and 30° are illustrated in Fig.8. These results show that increasing jet angle leads to a decrease of longitudinal velocity and an increase of radial velocity for the side jets.
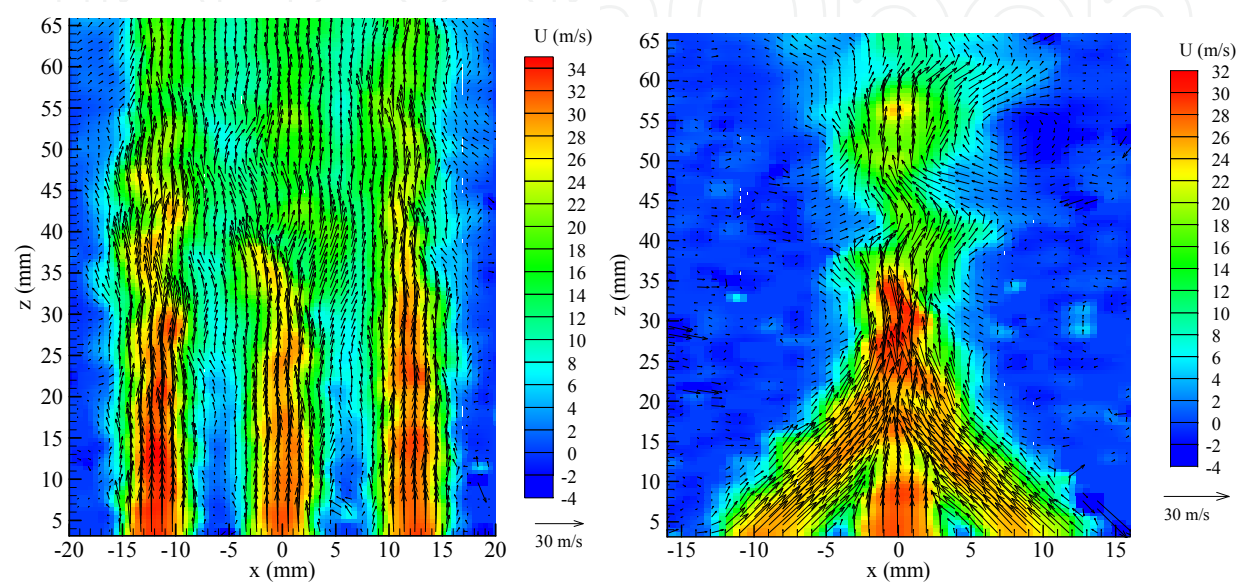
Fig. 7. Example of instantaneous velocity fields for θ = 0° (left) and θ = 30° (right) in non-reacting flow
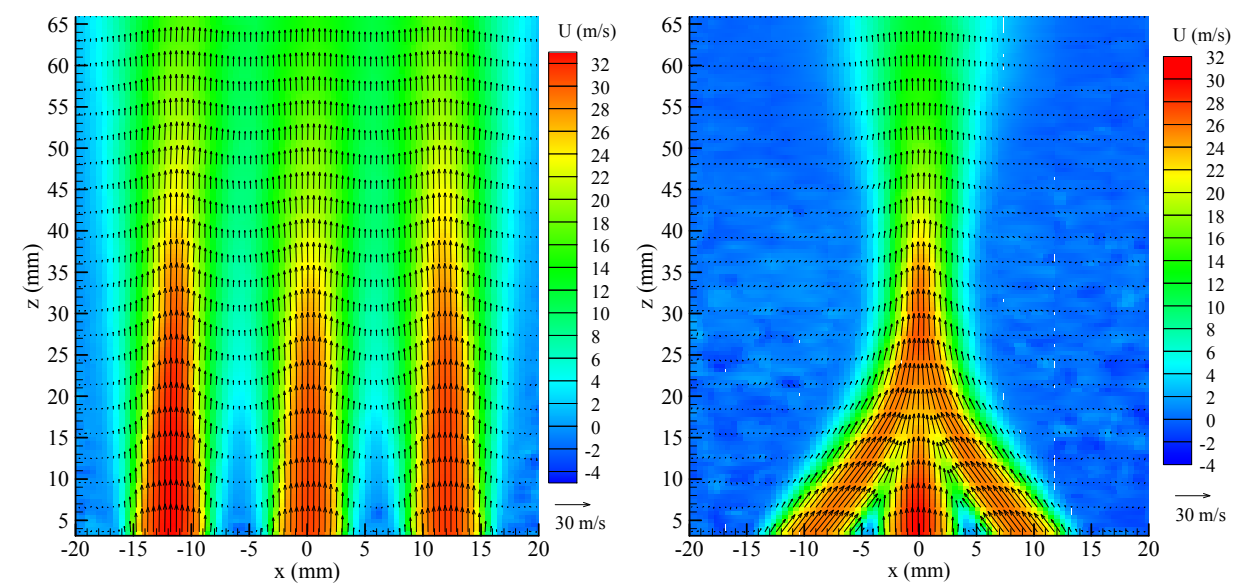
Fig. 8. Mean velocity fields for θ = 0° (left) and θ = 30° (right) in non-reacting flow (with longitudinal velocity in color scale)

From the initial state where θ=0° to inclined states, the structure of the dynamic field changes. As observed in the figure, the mixing of jets is more upstream for the inclined jet configurations. The merging region starts at 15 mm high for the straight jets (θ=0°), and more upstream for inclined jets, 7 mm for θ=10 ° and nearby to the burner for 20° and 30° (z=3 mm). The combined region, in which the velocity profiles combine to form a single jet profile, also starts much more upstream when the jets are angled. An increase of velocities between the jets with increasing jet angle is noted. At the height z=10 mm, the longitudinal velocity is zero between the jets for θ=0°, whereas it is around 12 m/s for θ=20°.

4.2 Radial profiles of mean velocities and fluctuations

Radial profiles of the mean longitudinal velocity (U) at different heights from the burner for the configurations θ = 0°, 10°, 20° and 30° are shown in Fig. 9. For the straight jets, a classical behavior of multiple jets is found for the distribution of longitudinal velocity, maxima in the centre of jets and minima between the jets. In the near burner region (e.g. z=15 mm), the distribution of velocity shows maxima and minima corresponding to the three jets and that
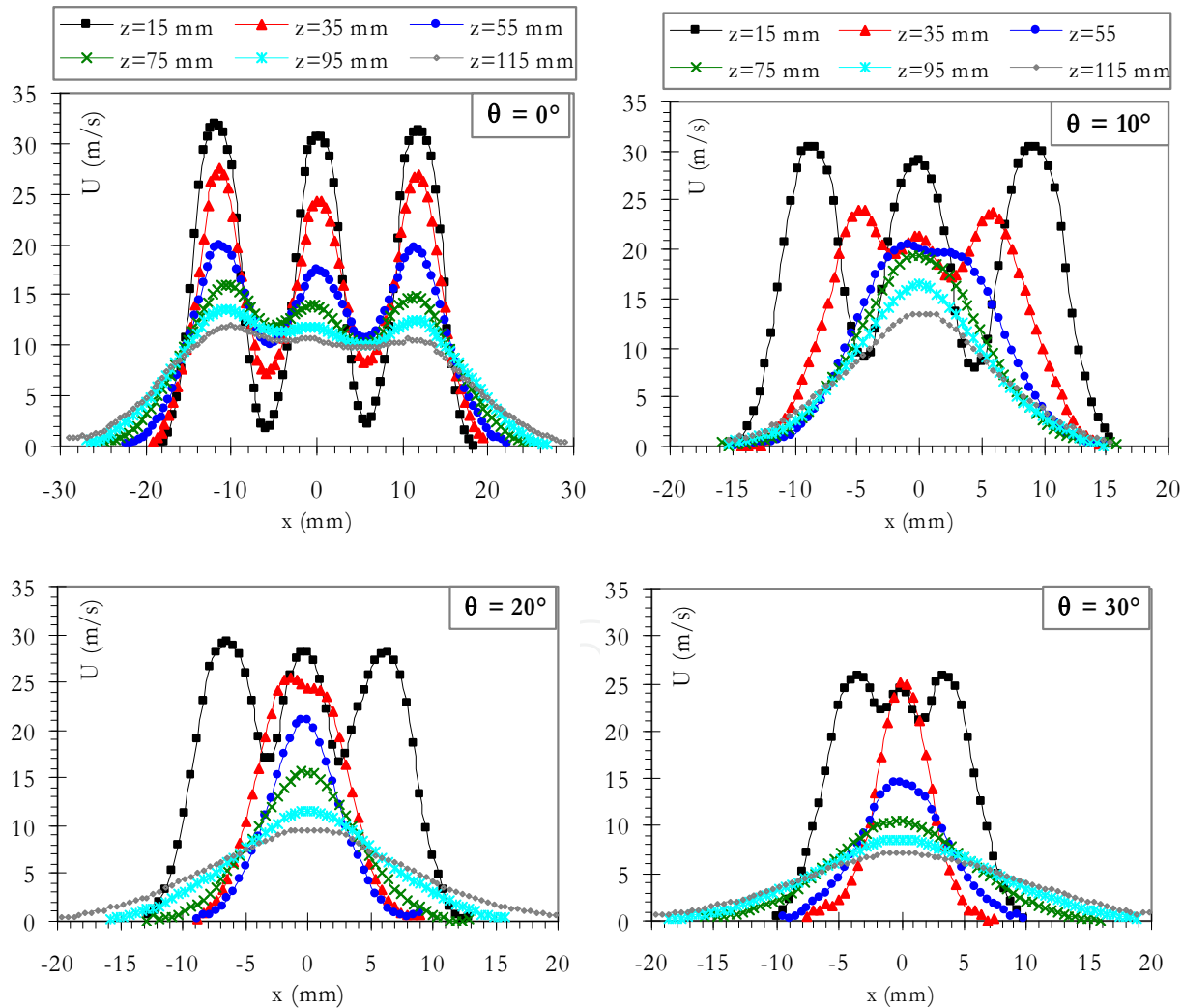

Fig. 9. Radial profiles of mean longitudinal velocity for jet angles 0°, 10°, 20° and 30° in non-reacting flow at different positions from the burner

the maximum velocity decreases when the jet angle increases. More downstream, when inclining the jets, the extreme velocities begin to disappear into a single maximum located along the axis of the center jet. This combined zone of jets, characterizing a single jet, is reached earlier when the jet angle increases.

Without control (θ=0°), the combined zone is not reached even at z=115 mm, while for θ=30° it is already occurred at z=35 mm. With control, in the combined zone it is noted an acceleration of the jet along the axis of the flow. In fact, at z=75 mm, from θ=0° to 10° the centerline longitudinal velocity (U) increases from around 15 to 19 m/s. However, once the combined region is reached, the velocity decreases with the angle of jets. The expansion of the flow decreases with the angle in the region near to the burner, and then increases downstream the flow.

The radial velocity profiles are shown in Fig.10 at different positions from the burner in non-reacting flow. For the straight jets (θ=0°), the radial velocity is low and ranges from -1 to 1 m/s. The deflection of jets leads to an increase of the radial velocity of the oxygen jets, particularly near the burner since at z=15 mm, the maximum value of V varies from 0.6 m/s
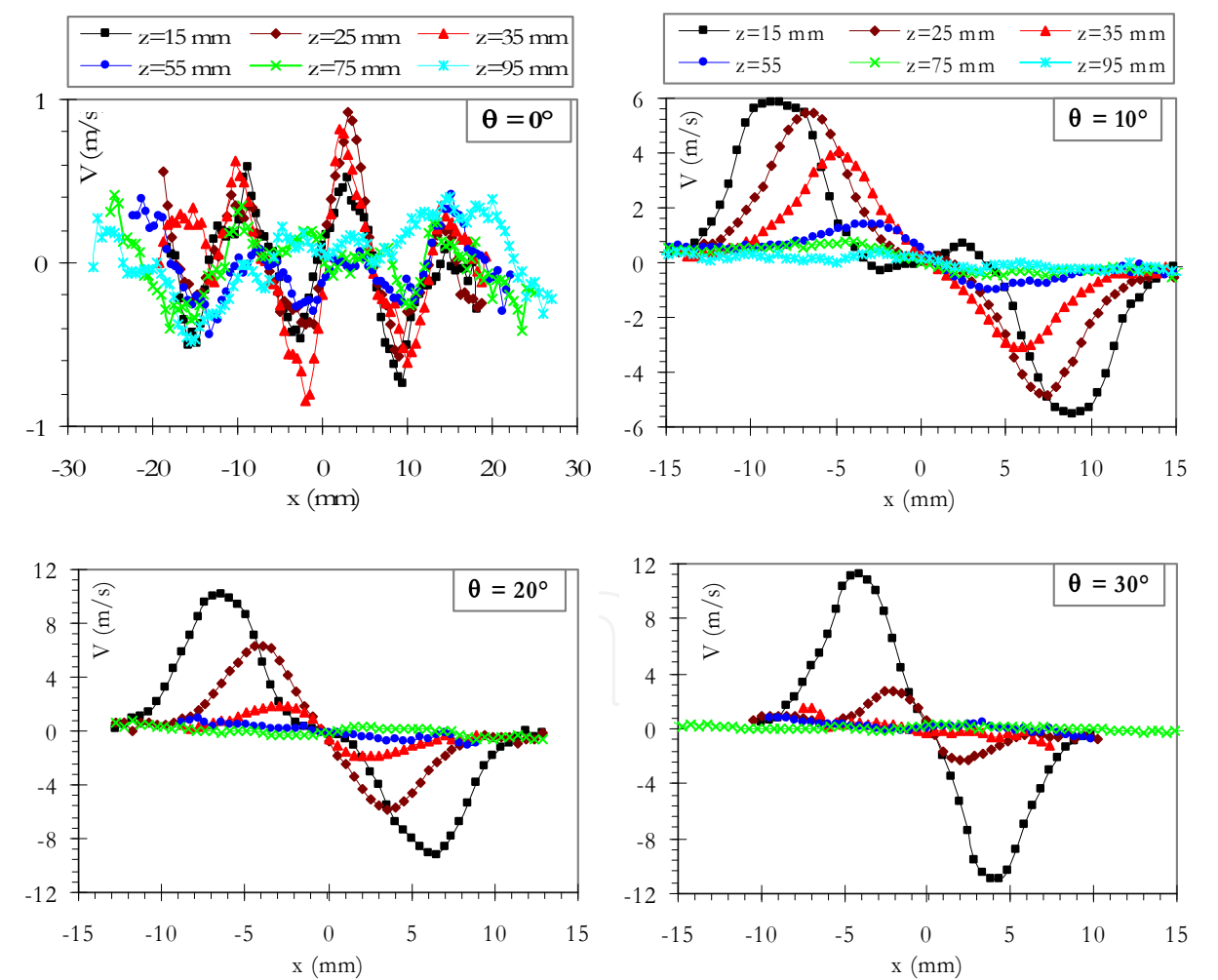

Fig. 10. Radial profiles of mean radial velocity for jet angles 0°, 10°, 20° and 30° in non-reacting flow at different positions from the burner

to 11 m/s when θ varies from 0° to 30°. For the inclined jets the velocity profile is composed of two parts, one positive and one negative with a passage by zero corresponding respectively to the side jets (left and right) and the central jet of natural gas.

Fig. 11 shows the radial distribution of the turbulence intensity (u'/U) with the jet angle at vertical positions z=15 and 75 mm. Results of u'/U highlight the interaction zones between the jets and surrounding air as well as between the jets themselves. In the initial region of flow (z=15mm), four zones of high turbulence are noticed. Two of them take place on the outer region of the side jets, involving a dilution of the oxygen jets by ambient air. The other two zones are located between the jets representing the jets mixing. Near the nozzle exits, the outer zones of turbulence do not seem to be affected by the increase of jet angle, while the inner zones decrease in intensity since the merging region is reached faster by the deflection of jets. Further downstream, when the jets merge, it is found that only the outer zones of turbulence behave as a single jet. At z=95 mm, except for straight jets, it is noted that whatever is the jet angle, the turbulence intensity profile u'/U is similar owing to the complete merging of jets at this position.
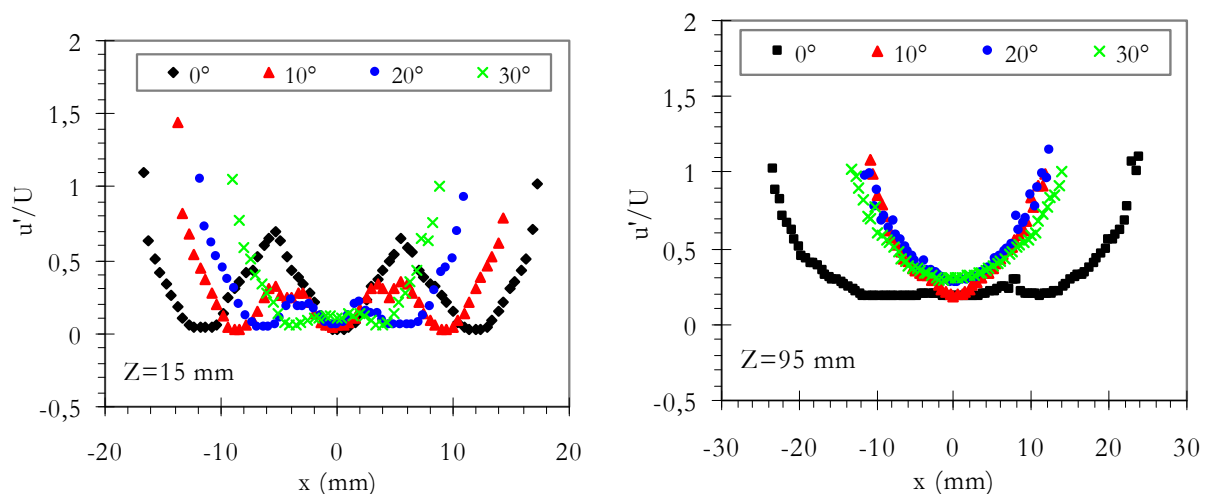

Fig. 11. Turbulence intensity (u'/U) at the vertical positions z=15mm and z=95mm for the jet angles 0°, 10°, 20° and 30° in non reacting flows

4.3 Velocities in oxy-fuel flames

Fig. 12 shows the mean velocity fields in the reacting flow (with combustion) for jet angles 0° and 30°. These vector fields show a significant difference between non-reacting and reacting flow. The first remark concerns the more significant velocities above the stabilization point in the reacting flow. Indeed, for the straight jets (θ=0°), the longitudinal velocity (U) decreases along the flow, however, this decrease is less significant compared to non-reacting flow. For the inclined jets, the longitudinal velocity in combustion keeps higher values even at more significant heights from the burner. The hot environment and the presence of a reaction zone lead to a fast expansion of gases due to the presence of flame, and therefore to an acceleration of the flow. The second remark concerns a greater radial expansion in combustion in particularly above the stabilization zone of the flame.
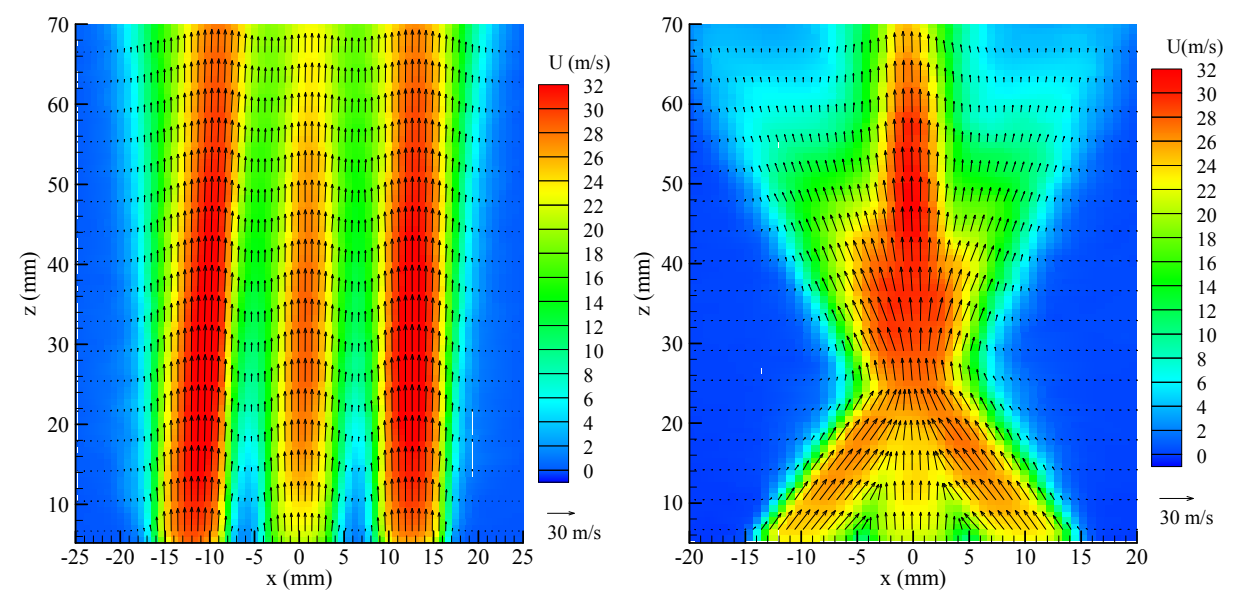
Fig. 12. Mean velocity fields for the oxygen jet angle θ=0° (left) and θ=30° (right) in reacting flow

The longitudinal velocities along centerlines (U_{cl}) in reacting and nonreacting flow are shown in Fig.13. The results concern the central jet of natural gas and one of the two side jets of oxygen for θ=0° and θ=20°. In the case of nonreacting flow, for the straight jets (θ=0°), the centerline velocity (U_{cl}) follows a classical decrease for the central and the side jets: first, a very slight decrease down to 26 mm corresponding to the potential core length of the jet, then a high decay of U_{cl} which corresponds to the merging of mixing layers, and finally a slow decay down to 65 mm for the natural gas jet and 75 mm for the oxygen jet. When the side jets are inclined (θ=20°, nonreacting), a decrease of the length of potential core is noted, and therefore a fast decrease of the longitudinal velocity appears in the first zone of the flow in particular for the central jet. After this first part of the flow, an increase of U_{cl} for the cases
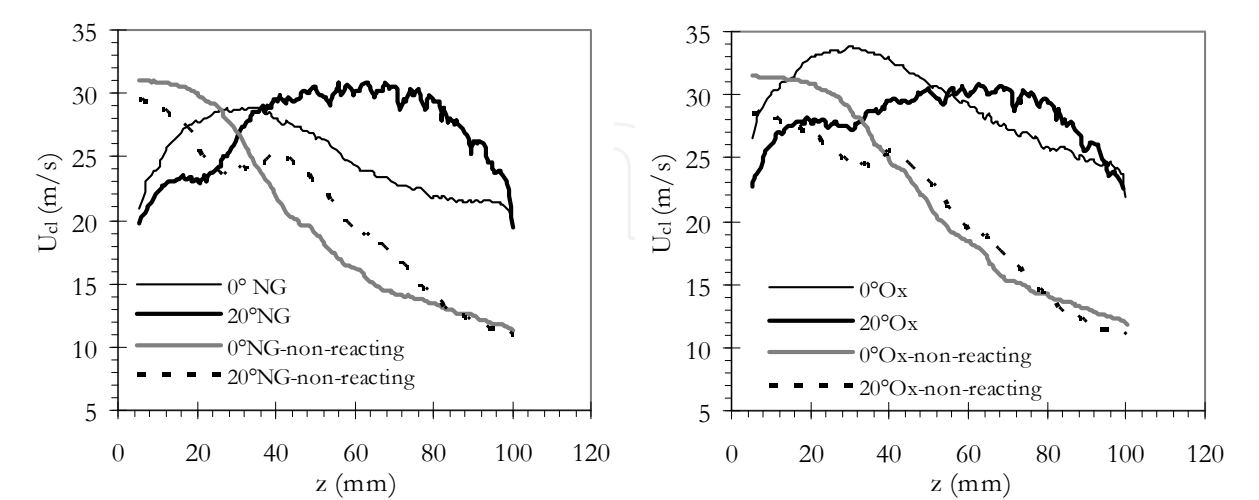

Fig. 13. Mean longitudinal velocity (U_{cl}) along the centerline of the central jet (left) and the side jet (right). A comparison between the reacting and the non reacting flow for the angles θ=0° and θ=20°

θ=20° at z=28 mm is observed. This behavior is attributed to the merging of three jets leading to an acceleration of flow at the beginning of the combined region.

In the case with combustion, the velocity U_{cl} increases with z distance in the first zone up to a maximum, then it conserves a high value, and finally, it slightly decreases along the centerline. The oxy-fuel combustion considerably influences the flow throughout the studied domain. In fact, in comparison with the non-reacting flow in the initial region, the flow is slower for both fluids, and then accelerates under the influence of high flame temperatures. For θ=20°, starting from z=40 mm, the centerline velocity is higher in the case of the reacting flow. After the stabilization point, the flow velocity is higher in the reactive case than that in the non reactive case. This is due both to the rapid expansion of burnt gases which accelerates the flow and to a retardation of mixing due to the presence of a flame.

5. PIV measurements on burners with swirling jets

5.1 Velocity fields in nonreacting flow

In order to examine the effects of the jet actuators on the flow, the case without control (*r*=0) and a case with a control parameter of *r*=0.15 are discussed (*r* represents the ratio of volumetric flow rates of actuators $\dot{m}_{act}$ and total $\dot{m}_{tot}$). Instantaneous velocity fields for the both configurations SW3J and SW2J (see Fig.3 and table 1) in the non reacting flow are shown in Fig. 14 and 16. The mean velocity fields are illustrated in Fig. 15 and 17. The instantaneous or mean fields clearly show the significant effect of the jet actuators on the flow structure. With the activation of actuation, the length of the potential core of the jets decreases and the longitudinal velocity decays more rapidly. This happens in favour of a high jet spreading and an enhancement of mixing, which furthermore leads to the flame stabilization more upstream, as previously indicated. This confirms the results previously reported in the literature on the efficiency of swirl on the mixing between the jet and the surrounding fluid (Syred and Béer, 1974; Faivre and Poinsot, 2004). Without control (r=0),
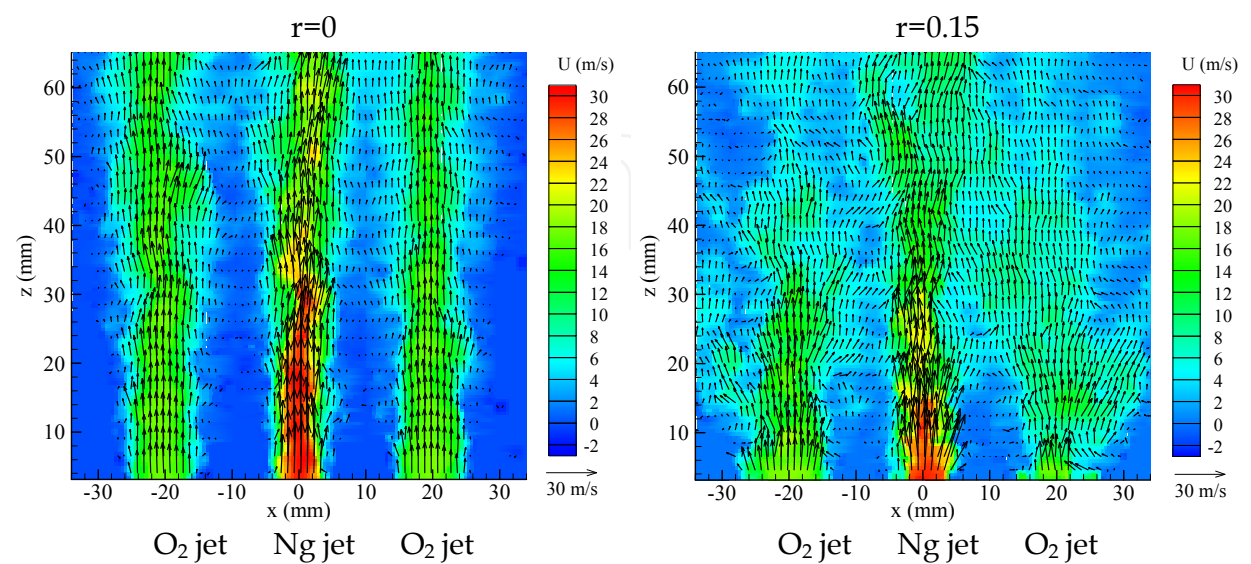

Fig. 14. Samples of instantaneous velocity fields for the flow rate ratio *r*=0 (without control) and *r*=0.15 (with control) in non-reacting flow for the SW3J configuration
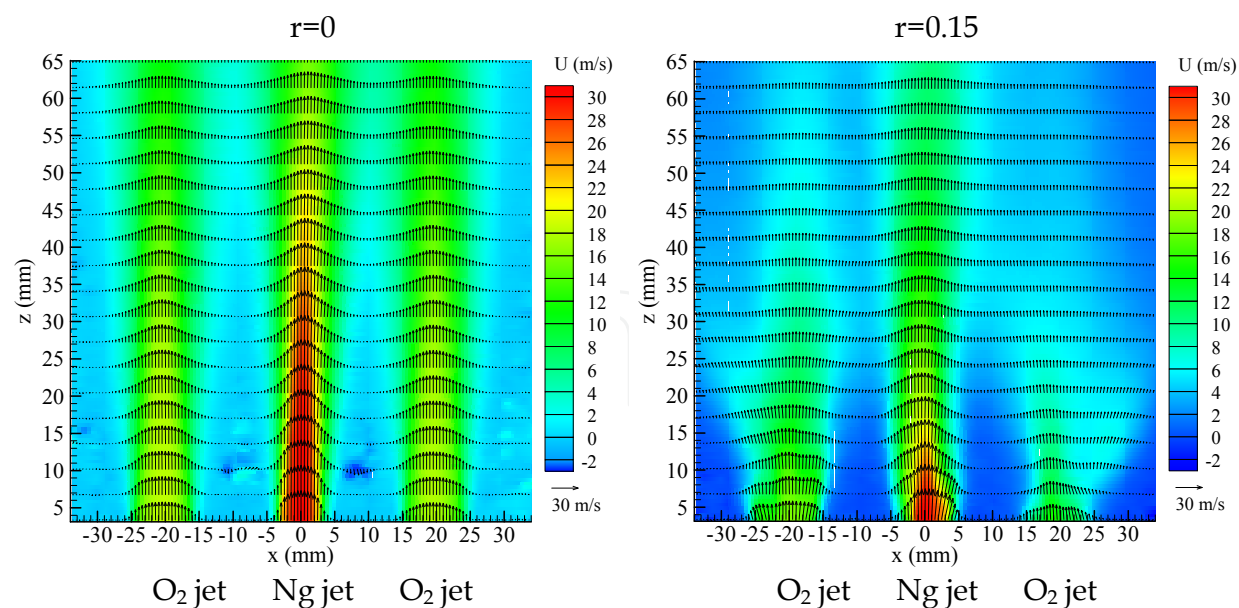
Fig. 15. Mean velocity fields for the flow rate ratio *r*=0 (without control) and *r*=0.15 (with control) in non-reacting flow for the SW3J configuration
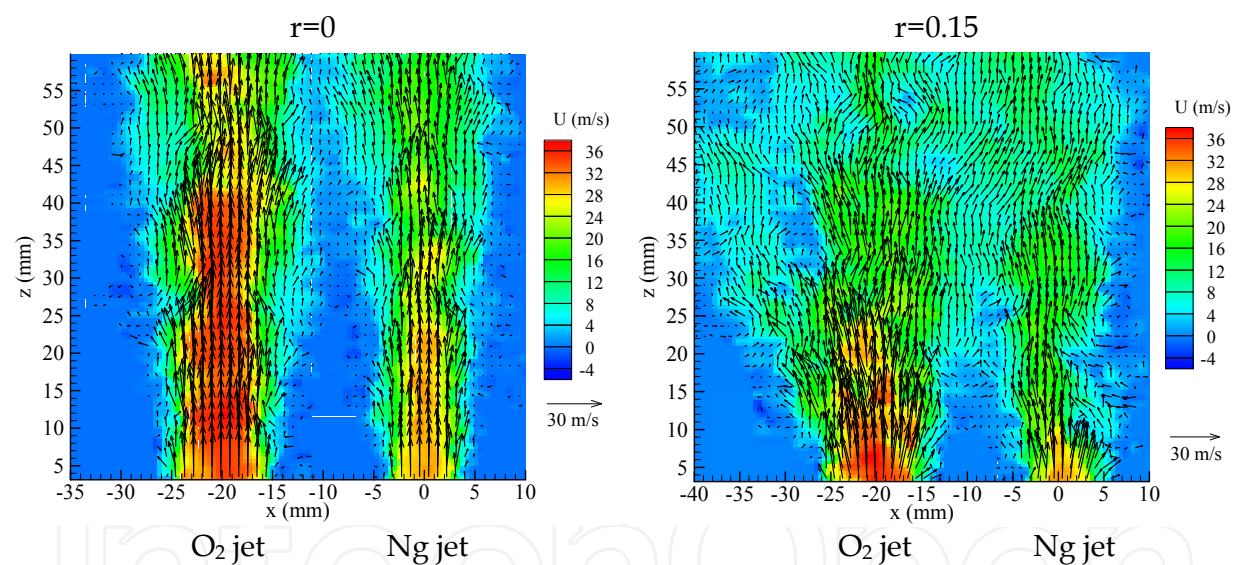

Fig. 16. Samples of instantaneous velocity fields for the flow rate ratio *r*=0 (without control) and *r*=0.15 (with control) in non-reacting flow for the SW2J configuration

the jets are well organized with a proper development for each jet in the initial zone of the flow and have a slight velocity variation at the centre. With control (r=0.15), instantaneous flow becomes highly disorganized and velocity gradients become important. In addition, the acceleration and the deflection of velocity vectors clearly appear in the whole field of view. The potential core of the controlled jets is definitely disturbed and its length decreases as a result of the jet actuators. For high swirl intensity (*r* > 0.2), the jets are more affected by the control, highly disorganized and develop also in the transverse plane (x,y); consequently the generated flame would be very oscillating and unstable (see Boushaki et al.2009). It is also noted the strong three-dimensional aspect of the flow, especially when using the jet

actuators, since many discontinuities in the velocity contours are observed. The mixing point (where the jets begin to interact) moves upstream in the flow with increasing r. In addition, when the distance (S) between the jets decreases, the mixing point gets closer to the burner.
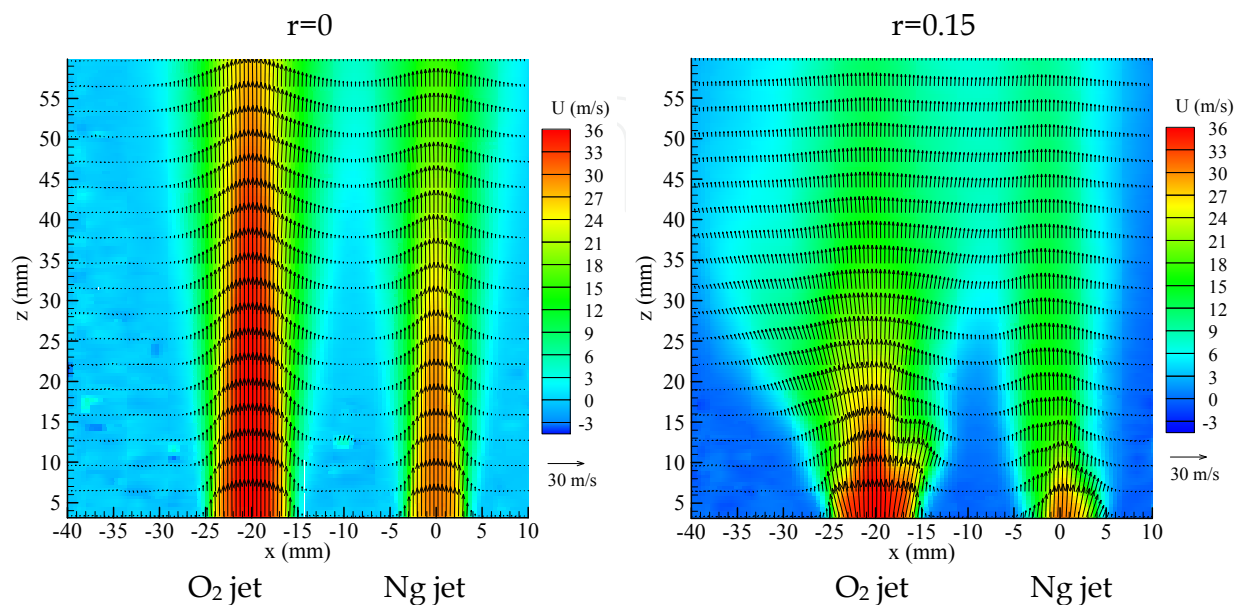

Fig. 17. Mean velocity fields for the flow rate ratio r=0 (without control) and r=0.15 (with control) in non-reacting flow for the SW2J configuration

Fig.18 shows radial profiles of the longitudinal and radial velocities at different heights from the burner, in the non reacting flow for the SW2J configuration. These profiles are presented for the both cases without control (r=0) and with control (r=0.15). Without jet actuators, the classical distribution of the longitudinal velocity in a multiple jet configuration is found, with maxima in the centre of the jets and minima between the jets. In the initial zone, each jet follows its own evolution, and then the jets start to interact. The activation of control jets changes the flow behavior and the distribution of jet velocities. The control leads to a faster velocity decay and alters the shape of radial profiles near the burner. Indeed, at z = 35 mm for example, the maximum longitudinal velocity is 34 m/s without control, whereas in the controlled configuration it is 17 m/s. The control also accelerates the longitudinal velocity decay, as expected in as swirling flow. Near the injector exits (z=5 mm), it is observed that the maximum velocity remains high and even slightly higher when r increases. It can be explained by the involvement of the tangential velocity component, which increases with the flow rate control and compensates the decrease induced in main jets when r increases. This situation was also observed in the work of Faivre and Poinsot (2004) on a single jet. Furthermore, the asymmetry of the velocity profiles in the initial zone of flow induced by the tangential activation of control jets is observed. Far from the burner, this asymmetry however disappears and the profiles become axisymmetric.

The influence of the jet actuators on the flow behaviours also concerns the other velocity components, in particular in the initial zone of the flow. Fig.18.c-d shows that the radial velocity increases in the case of controlled jets. Without control, V is low ($-1 \leq V \leq +1$ m/s), whereas with control the maximum radial velocity can reach 6 m/s for r=0.15 and 12 m/s for r=0.2 near the burner.

a) U ($r = 0$)

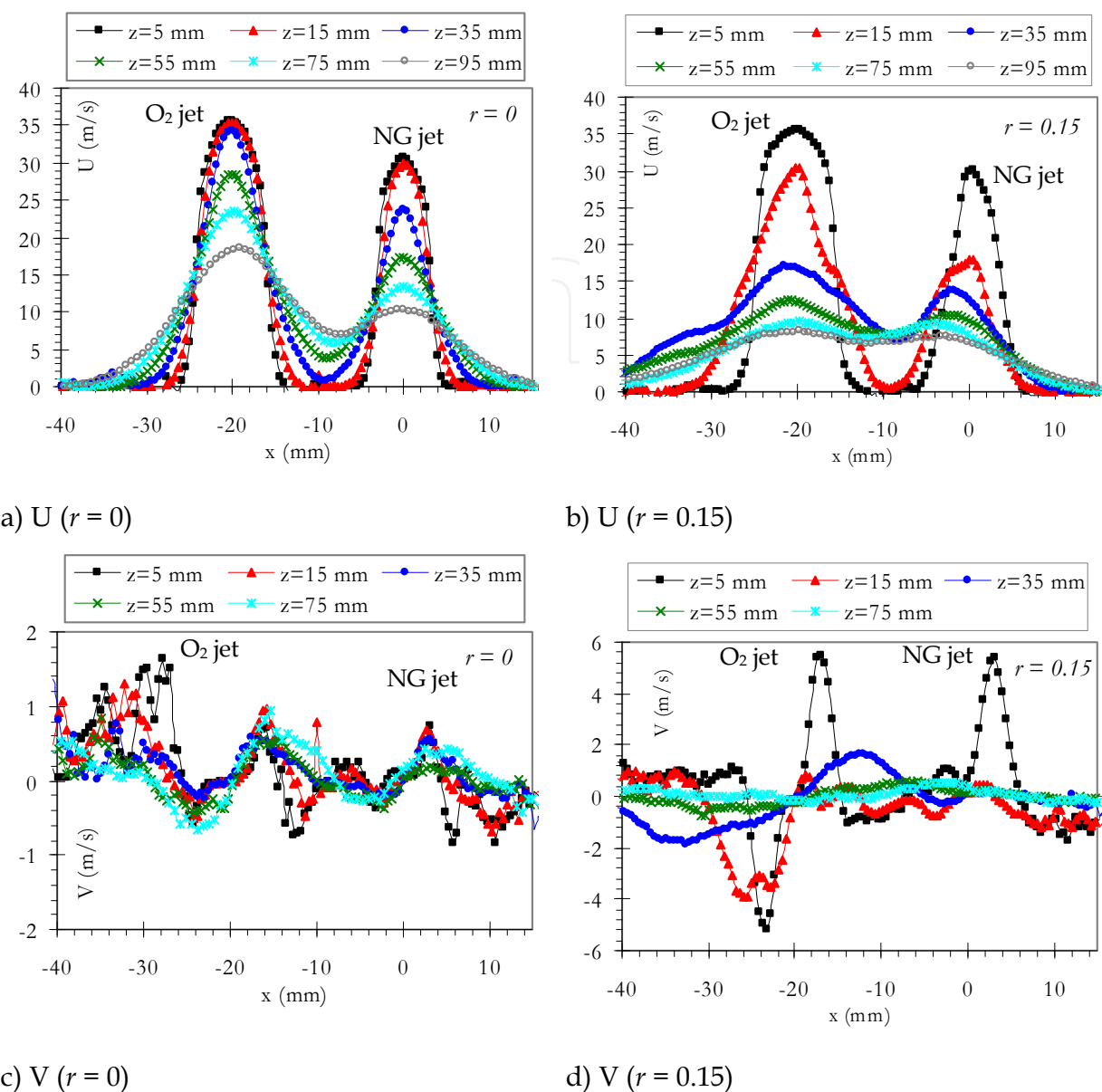b) U ($r = 0.15$)

c) V ($r = 0$)

d) V ($r = 0.15$)

Fig. 18. Radial profiles of mean velocities for the SW2J configuration in the non reacting flow, without control (r=0) and with control (r=0.15); a-b) longitudinal component (U), c-d) radial component (V).

5.2 Axial profiles of mean velocities

Fig.19 shows longitudinal velocities along centrelines of natural gas and oxygen jets for the flow rate ratios r=0, 0.1, 0.15 and 0.2 in the non-reacting flow for the SW2J configuration. Without control, the velocity evolution along the centreline (U_{cl}) is almost similar to the one of a simple jet. First, it can exhibit a plateau corresponding to the potential core of the jet, followed by a pronounced decay of U_{cl} (mixing layers merging), and finally a slow decay. It is noted that the initial plateau is longer for the oxygen jet on account of greater jet diameter (d_{ox}= 8 mm, d_{ng}= 6 mm) with a slight difference in injection velocities of the two fluids.
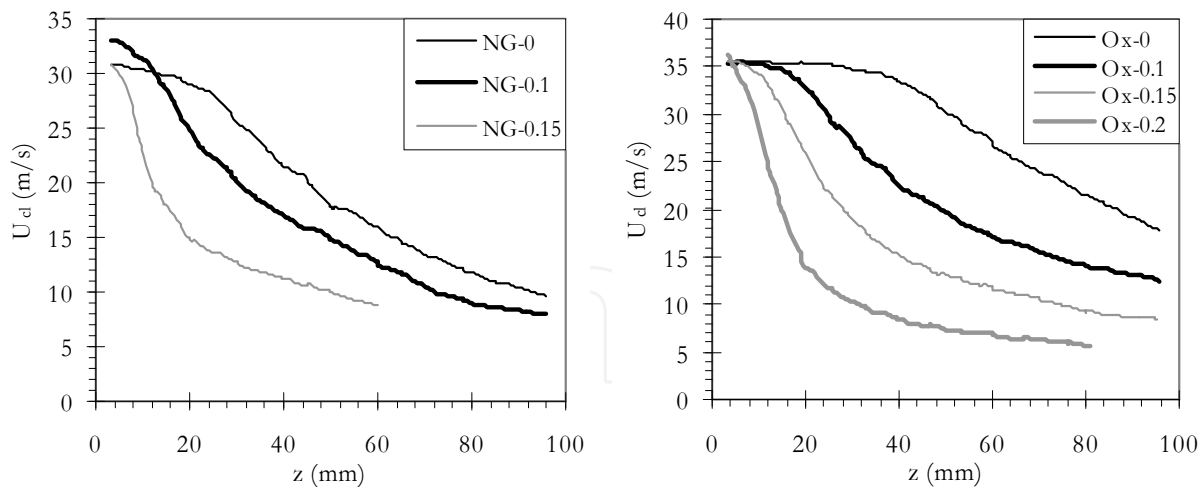
Fig. 19. Mean longitudinal velocity along the centerline of the natural gas jet (left) and the oxygen jet (right) for flow rate ratios (r), 0, 0.1, 0.15 and 0.2. Case: configuration SW2J, non-reacting flow

The activation of control jets changes the flow behaviour and the distribution of jet velocities. The decrease of centreline velocity is faster near the burner, and then it further slows downstream. It appears that the greater the flow rate ratio is, the higher the centreline velocity decays. Another important element concerns the potential core of jets, which is strongly affected by the control. Indeed, for r=0.1, the length of the potential core is very small compared to the cases without actuators. Between the two cases (r=0 and 0.1), the length of the potential core for the oxygen jet decreases from $4d_{ox}$ to $2.25d_{ox}$. Over for r=0.1, the plateau of the potential core is completely disappeared and the centres of jets are reached closer to the exit nozzles, which is caused by jet actuators impacting the main jets with high velocities.

5.3 Radials profiles of velocity fluctuations

The radial profiles of rms velocities, u′ (longitudinal velocity fluctuations) and v′ (radial velocity fluctuations) for the SW2J configuration at various heights of the flow with and without control are shown in Fig.20. The results indicate the significant effect of the jet actuators, since the intensity of velocity fluctuations increases in the case r=0.15. In the case without actuators, the radial distribution of u′ and v′ with peaks of turbulence is found. The maximum values of u′ are obtained close to the burner, and are of about 6 and 7 m/s for natural gas jet and oxygen jet, respectively (a and c). Further downstream, the intensity of the fluctuations is attenuated in turbulence zones. Indeed, at z=75 mm, u′ is about 3 and 4 m/s in the natural gas and oxygen jets, respectively. In the case with actuators, the values of u′ and v′ are more significant (b and d). In fact, for r=0.15, the maximal values of u′ are 10 and 6 m/s for the fuel and oxidizer. For z=15 mm, a high increase of fluctuations appears along the jets axis, affected by the tangential jets. This shows the increase of turbulence zones near the nozzle exits, favouring mixing with the ambient air and between the jets themselves.

The control effect on the fluctuations of radial velocity (v′) is more pronounced as shown in Fig.20.d. The fact of introducing tangentially a portion of jet flow rate tends to influence the initial zone of the flow and induces high radial velocity fluctuations. It is shown that maximum values of v′ are of the order of 4 to 5.5 m/s with actuators (d), instead of 1.5 to 2.5 m/s for the case without jets actuators (c) in the zone close to the burner.
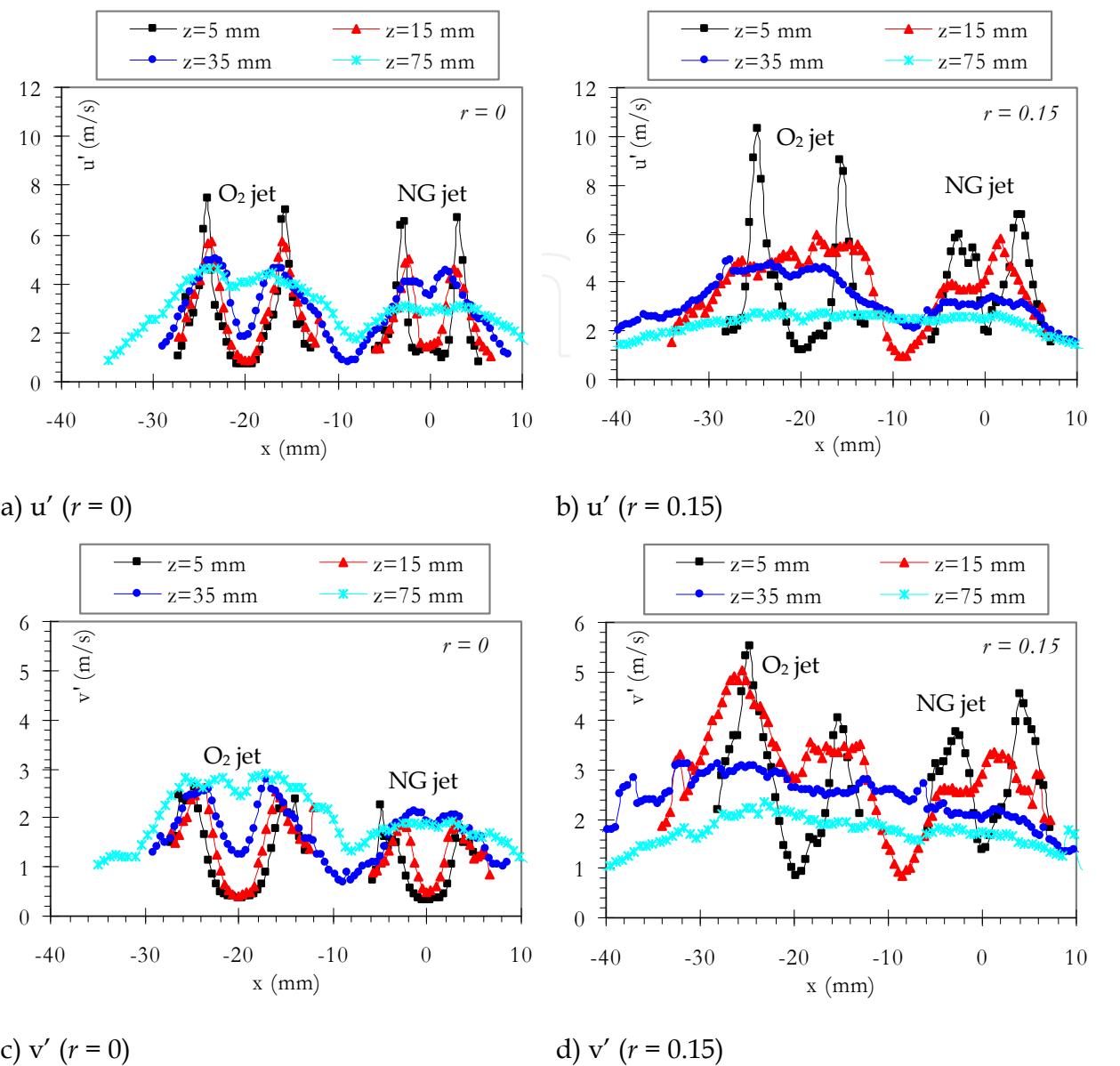
a) u′ (r = 0)

b) u′ (r = 0.15)

c) v′ (r = 0)

d) v′ (r = 0.15)

Fig. 20. Radial profiles of rms velocities for the SW2J configuration in non reacting flows without control (r=0) and with control (r=0.15); a-b) longitudinal velocity fluctuations (u′), c-d) radial velocity fluctuations (v′)

5.4 Velocity fields in oxy-fuel flames

In this section, the measurements of velocities in oxy-fuel combustion by PIV technique in the furnace are presented. Fig.21 shows the mean velocity fields (with the longitudinal velocity in color scale) for the SW2J configuration without control (r=0) and with control (r=0.15). The radial profiles are shown in Fig.22. These results indicate that the velocity field is also affected by the use of jet actuators. In the presence of jet actuators, a higher decrease and wider spreading of the flow are observed when the flow rate control r increases. The merging and combined zones of the jets occur more and more upstream with increasing r. Therefore, the stabilization point (small squares in pink color in the figure) of the flame

moves upstream with the control and locates in the zone inter-jets where the velocity is low. Note that the stabilization point has been deduced from OH* emission measurements (see Bouhaki et al. 2009) and represents the region where the combustion starts. Without actuators (*r*=0), the flow velocity decreases along the axis but this decrease is slower than in the case of non-reacting flow, in particular for oxygen jet. Between z=5 mm and 95 mm, the maximum velocity of the oxygen jet decreases from 33 to 27 m/s, whereas in non-reacting flow, the maximum velocity passes from 36 to 18 m/s. In non-reactive flow, mixing and turbulence develop faster which generates a faster decrease of velocity. It is shown that in the initial zone of the flow, the maximal velocity is higher in non-reacting flow than in the reacting flow. The velocity profiles in combustion are slightly more flattened and more open, due to the high heat release from oxy-fuel flame. With control, the longitudinal velocity decay and radial spreading are more significant when the flow rate ratio *r* increases. As in the case without control, the velocity decay is slower with control in the reacting flow compared to the non-reacting flow. Above the stabilization point, the flow keeps a higher velocity owing to the fast expansion of hot gas by the reaction. As an example, for z=55 mm, the maximum velocity of reacting flow is about 21 against 12 m/s in the non-reacting flow. The presence of flame may decrease the entrainment of ambient fluid, which accelerates the flow. This result was observed by Takaji et al. (1981) on a turbulent H_2-N_2/Air flame by comparison between non-reacting and reacting flow.

The enhancement of mixing by the jet actuators leads to a decrease in lift-off heights and a better stability of the flame as shown in Boushaki et al. (2009). However, the flame length decreases with the flow rate of jet control since the mixing is improved by using swirling flow. In practical systems the flame length is an important factor since it defines the distance on which the heat transfer is transmitted. On the other hand, for this control system in the range $0 \leq r \leq 0.2$, the flame length remains relatively higher. Moreover, in this range of low flow rate ratio, globally NOx production decreases when *r* increases.
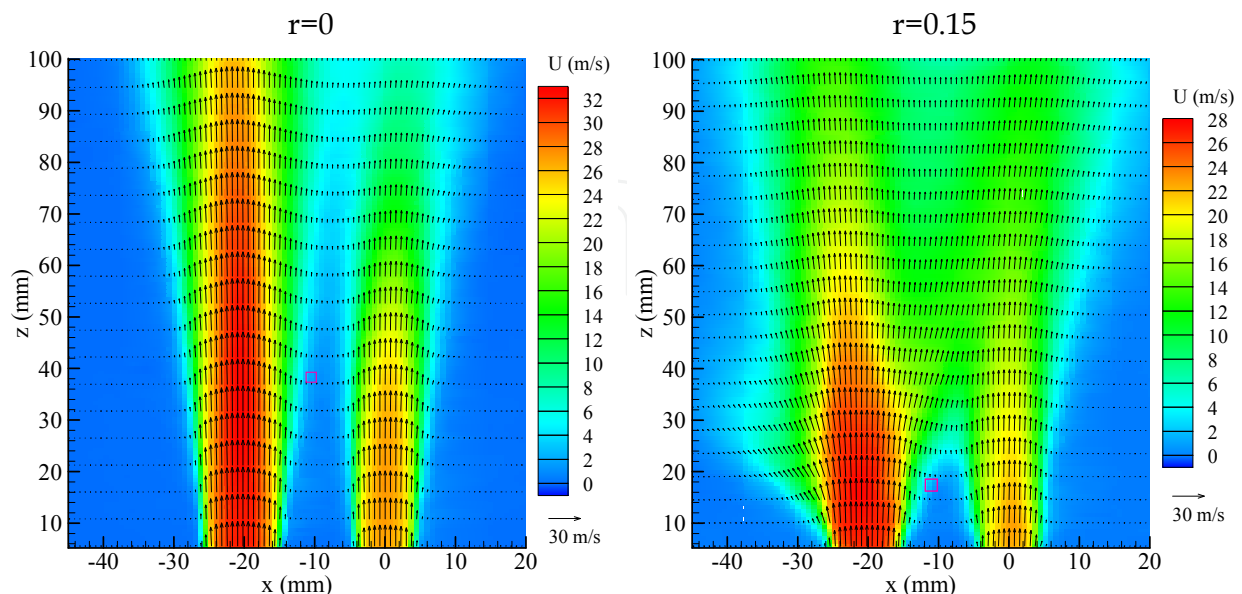

Fig. 21. Mean velocity fields for the SW2J configuration in reacting flow, without control (left) and with control. The point in pink color represents the position of the flame base
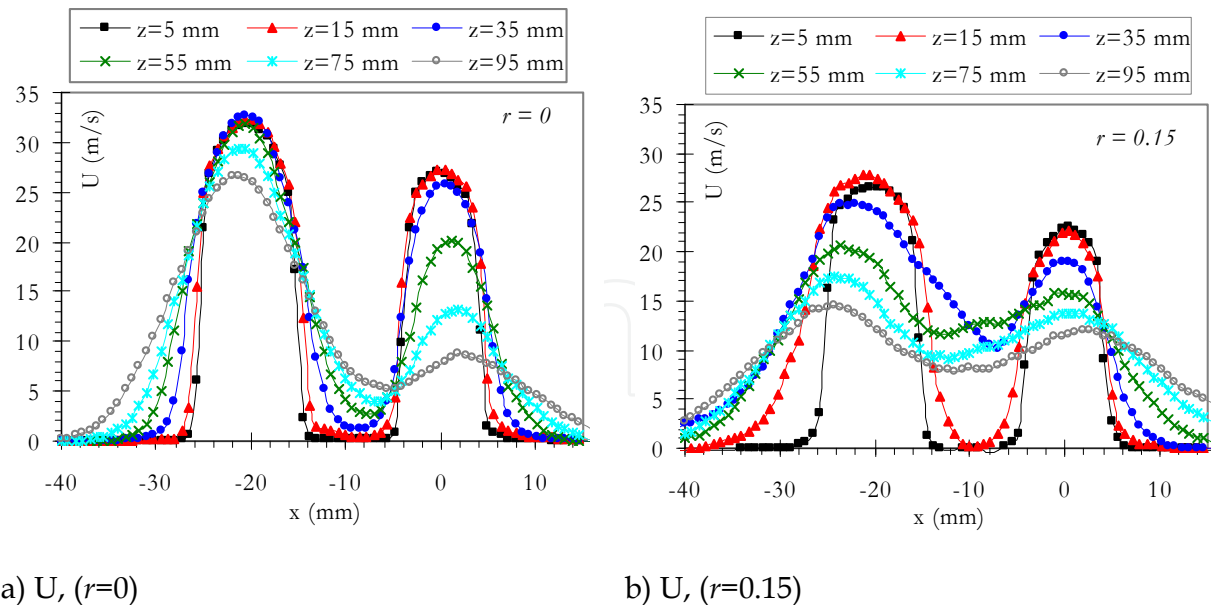
a) U, (*r*=0)   b) U, (*r*=0.15)

Fig. 22. Radial profiles of mean longitudinal velocity for the SW2 configuration in reacting flow, a) without control (*r*=0), b) with control (*r*=0.15).

6. Conclusion

The dynamic study by PIV measurements on oxy-fuel burners with separated jets is investigated in this chapter. Measurements by PIV technique enable the characterization of the behavior and structure of jets and the distribution of velocity fields. Particular attention has been paid to the particle seeding, oil particles for non-reacting configuration and solid ZrO_2 particles in combustion. The measurements of the velocity fields are fulfilled on a burner composed of three jets, one central jet of natural gas and two side jets of pure oxygen. Measurements concern the nonreacting flow and the reacting flow in turbulent diffusion flames inside a combustion chamber. Two types of control of flows are developed and applied on the basic configuration of burner. A passive control based on the deflection of jets, and an active control that consists of four small jet actuators, placed tangentially to the exit of the main jets to generate a swirling flow.

Results of passive control show that the inclination of side jets towards the central jet improves the mixing and thus accelerates the merging, and then the combining of jets where velocity profiles become uniform to form a single jet profile. The deflection of injectors induces a radial velocity in the first zone of flow increasing with the jet angle. Along the flow, this velocity decreases since the side jets impact the central jet and the flow forms a single jet. With deflection of jets, the potential core length decreases, and therefore the longitudinal velocity decreases rapidly in the first zone of the flow with the jet angle. The oxy-fuel combustion generates significant changes on the distribution of the dynamic fields. The velocities are higher compared to non-reacting flow, in particular above the stabilization region. This is due both to the rapid expansion of burnt gases which accelerates the flow and a retardation of mixing due to the presence of the flame. Also, a greater radial expansion in reacting flow, particularly above the lift-off position of flame, was observed.

The results about the active control show that the presence of tangential jet actuators appreciably acts on the structure of the flow and consequently on the flame behaviour. The control by jet actuators induces a decrease in the length of potential core of jets, more important spreading of flow and higher longitudinal velocity decay. It is observed that for r (flow rate ratio) > 0.1 the potential core disappears completely due to the jet actuation. The center of the jet is reached closer to the exit of nozzles as a result of jet actuators that impact with high velocity the main jets. Moreover, the increase of control flow rate accelerates the merging of the jets and the flow rapidly reaches the characteristics of a single jet. Near the burner, the transverse velocity increases with the control and can reach 10 m/s due to the tangential injection by actuators. Velocity fluctuations (longitudinal and radial) increase with the control, and therefore the layers of turbulence widen significantly and promote mixing with the ambient medium and between the jets themselves. From non controlled jets ($r=0$) to controlled jets ($r>0$), the turbulence intensity along the jet axis highly increases, in particular near the exit of jets (from 5 to 25% in the configuration SW2J). Measurements in combustion revealed some changes on the flow velocity fields. The dynamic development of oxy-fuel flame is highly slowed by the presence of the high temperature environment, since the decrease in velocities is slower compared to the nonreactive case. The evolution of the longitudinal velocity shows that even in the presence of control, the values of U_{cl} remain high near the burner, and then decrease slowly along the flow development.

7. Acknowledgment

8. References

Ahuja, K.K. (1993). Mixing enhancement and jet noise reduction through tabs plus ejectors. *AIAA Paper*, 93-4347.

Barrère, M. & Williams, F. (1968). Comparison of Combustion Instabilities found in Various Types of Combustion Chambers, *Proceedings of the Combustion Institute*, 12, pp. 169-181.

Baukal, CE. & Gebhart, B. (1997). Oxygen-enhanced/natural gas flame radiation. *International Journal of Heat and Mass Transfer* 40(11): 2539-2547.

Baukal, CE. (2003). Industrial burners handbook, CRC Press

Beér, J. M. & Chigier N. A. (1972). Combustion Aerodynamics, ed. Krieger, Malabar, Florida.

Bloxsidge, G J; Dowling, A P.; Hooper, N. & and Langhorne, P.J. (1987) Active control of an acoustically driven combustion instability *J. Theor. Appl. Mech.* 6, pp. 161–75.

Boushaki, T.; Sautet, J.C; Salentey, L. & Labegorre, B. (2007)., The behaviour of lifted oxy-fuel flames in burners with separated jets, *International communication in Heat and Mass Transfer*, 34, pp 8-18.

Boushaki, T; Mergheni, M-A. ; Sautet, JC. & Labegorre, B. (2008). Effects of inclined jets on turbulent oxy-flame characteristics in a triple jet burner, *Exp. Therm. Fluid Sci.* 32:1363-1370.

Boushaki, T; Sautet, JC. & Labegorre B. (2009). Control of flames by radial jet actuators in oxy-fuel burners, Combustion and Flame, *Combustion and Flame*, 156, 2043–2055.

Bradbury, L.J.S. & Khadem, A.H. (1975). The distortion of a jet by tabs. *Journal of Fluid Mechanics*, 70, 801–813.

Candel S. (1992). Combustion Instabilities Coupled by Pressure Waves and Their Active Control, *Proceedings of the Combustion Institute* 24, pp. 1277-1296.

Coghe, A.; Solero, G. & Scribano, G. (2004). Recirculation phenomena in a natural gas swirl combustor, *Experimental Thermal and Fluid Science*, 28, pp. 709-714.

Davis, A. & Glezer, A. (1999). Mixing control of fuel jet using synthetic jet technology : velocity field measurements, *37th AIAA Aerospace Sciences Meeting and Exhibit Reno*, NV, AIAA 99-0447, pp. 1-15.

Davis, M.R. (1982). Variable control of jet decay, *AIAA Journal*, 20, pp. 606-609.

Delabroy, O.; Haile, E.; Veynante, D.; Lacas, F. & Candel S. (1996), Réduction de la Production des Oxydes d'Azote (NOx) dans une Flamme de Diffusion à Fioul par Excitation Acoustique, *Revue Générale de Thermique* 35, pp. 475-489.

Demayo, T.N.; Mcdonell, V.G. & Samuelsen, G.S. (2002). Robust Active Control of Combustion Stability and Emissions Performance in a Fuel-staged Natural-gas-fired Industrial Burner, *Proceedings of the Combustion Institute* 29, pp. 131-138.

Denis, S.; Delville, J. ; Garem, J.H. & Bonnet, J.P. (1999). Contrôle de l'expansion d'un jet rond par des jets impactants. *14ème Congrès Français de Mécanique*, pp. 1-6.

Faivre, V. & Poinsot, T. (2004). Experimental and numerical investigations of jet active control for combustion applications, *Journal of Turbulence* 5, 025.

Feikema, D.; Chen, R.H. & Driscoll J.F., Enhancement of flame blowout limits by the use of swirl, *Combustion and Flame*, 80:183-195, (1990).

G.E.F.G.N. (1983). Utilisation de l'oxygène dans les flammes de diffusion de gaz naturel. *Revue Générale de Thermique.*, N° 214, pp: 643-649

Gollahalli, S; Khanna, T. & Prabhu, N. (1992). Diffusion Flames of Gas Jets Issued From Circular and Elliptic Nozzles. *Comb. Sci. Technol.* 86, pp. 267-288.

Gutmark, E.J., Grinstein, F.F., (1999). Flow control with noncircular jets. *Annual Review of Fluid Mechanics* 31, pp. 239–272.

Hileman, J.; Caraballo, E. & Samimy, M. (2003). Simultaneous real-time flow visualizations and acoustic measurements on a tabbed Mach 1.3 jet. *AIAA Paper* 2003-3123.

Ho, C., Gutmark, E.J., (1987). Vortex induction and mass entrainment in small-aspect-ratio elliptical jet. *Journal of Fluid Mechanics* 179, pp. 383–405.

D. Honoré, S. Maurel, A. Quinqueneau, "Particle Image Velocimetry in a semi-industrial 1 MW boiler", *Proceedings of the 4th International Symposium on Particle Image Velocimetry*, Göttingen, Germany, Sept. 11-19, 2001.

Ibrahim, M.; Kunimura, R. & Nakamura, Y. (2002). Mixing enhancement of compressible jets by using unsteady microjets as actuators, *AIAA J.* 40 681–8.

Ivernel, A. & Marque, D. (1975). Flammes industrielles de gaz naturel. Influence de la suroxygénation du comburant. *2nd Europeen Combustion Symposium*, pp 121-128

Krothapalli A.; Bagadanoff D. & Karamchetti K. (1980). Development and structure of a rectangular jet in a multiple jet configuration, *AIAA journal*, vol 18, N° 8, pp 945-950, (1980).

Krothapalli A.; Bagadanoff D. & Karamchetti K. (1980). Development and structure of a rectangular jet in a multiple jet configuration, *AIAA journal*, vol 18, N° 8, pp 945-950, (1980).

Lang, W.; Poinsot, T. & Candel, S. (1987). Active control of combustion instability, *Combustion and Flame*, 70, pp. 281-289.

Lardeau, S.; Lamballais, E. & Bonnet, J.P. (2002). Direct numerical simulation of a jet controlled by fluid injection, *Journal of Turbulence*, 3.

Lecordier B., Trinité M. (2003). Advanced PIV algorithms with image distortion validation and comparison using synthetic images of turbulent flow, *Particle Image Velocimetry: recent improvement*, Springer.

Lee, B-J.; Kim, J-S. & Lee, S. (2004). Enhancement of blow-out limit by the interaction of multiple nonpremixed jet flames, *Combust. Sci. and Tech*, 176, pp. 481-497.

Leite, AOP.; Ferreira, MA. & Carvalho, JA. (1996). An investigation of multiple jet acetylene flames. *International Communications in Heat and Mass Transfer* 23 (7): 959-970.

Lenze, B.; Milano, ME.; & Günther, R. (1975). The mutual influence of multiple jet diffusion flames. *Combust. Sci. and Tech.*, 11:1-8.

McManus, K.R; Poinsot, T. & Candel, S. (1993). A Review of Active Control of Combustion Instabilities, *Progress in Energy and Combustion Science,* 19, pp. 1-29.

Menon, R. & Gollahali, SR. (1998). Combustion characteristics of interacting multiple jets in cross flow. *Combust. Sci. and Tech.*, 60:375-389.

Moawad Ahmed K.; Rajaratnam, N. & Stanley, SJ. (2001). Mixing with multiple circular turbulent jets. *Journal of hydraulic research*, vol. 39, N°2: pp. 163-168.

Pani, B. & Dash, R. (1983). Three dimensional single and multiple jets. *J. Hydr. Engrg,* 109 (2): 254-269.

Perthuis, E. (1983). La combustion industrielle. Editions Technip, Paris

Raffel, M.; Willert, CE. & Kompenhans, J. (1998). Particle Image Velocimetry, A Practical Guide, Springer ed. ISBN-10: 3540636838.

Raghunatan, S. & Reid, I.M. (1981). A study of multiple jet. *AIAA paper* 19, 124-127

Sautet, JC; Boushaki, T.; Salentey, L. & Labegorre, B. (2006). Oxy-combustion properties of interacting separated jets. *Combust. Sci. and Tech.*, 178: 2075-2096.

Schmittel, P.; Günther, B.; Lenze, B.; Leuckel, W. & Bockhorn, H. (2000). Turbulent swirling flames: experimental investigation of the flow field and formation of nitrogen oxide, *28th Symposium (International) on Combustion*, pp 303-309.

Sheen H.J; Chen, W.J.; Jeng, S.Y.; Huang, T.L. (1996). Correlation of swirl number for a radial-type swirl generator. *Experimental Thermal and Fluid Science* 1996; 12: pp 444-451.

Simonich JC (1986) Isolated and interacting round parallel heated jets. AIAA paper 86-0281

Strahle, W.C. (1978). Combustion Noise. *Pro. Energy Combust. Sci.*, 4, pp. 157-176.

Susuki, H; Kasagi, N. & Susuki, Y. (1999). Active control of an axisymmetric jet with an intelligent nozzle *Proc. 1st Int. Symp. on Turbulent Shear Flow (Santa Barbara),* pp 665–70.

Syred N. & Béer J.M. (1974). Combustion in swirling flows : A review, *Combustion and Flame*, 23:143-201.

Takagi, T., Shin, H.D. & Ishio, A. (1981). Properties of turbulence in turbulent diffusion flames, *Combustion and Flame*, 40:121-140.

Tamburello, DA. & Amitay, M. (2008). Manipulation of an Axisymmetric Jet by a Single Synthetic Jet Actuator. *International Journal of Heat and Fluid Flow* 29, pp. 967-984.

Yimer, I.; Becker, HA. & Grandmaison, EW. (1996). Development of flow from multiple jet burner, *A.I.C.H.E Journal* 74, pp. 840-851.
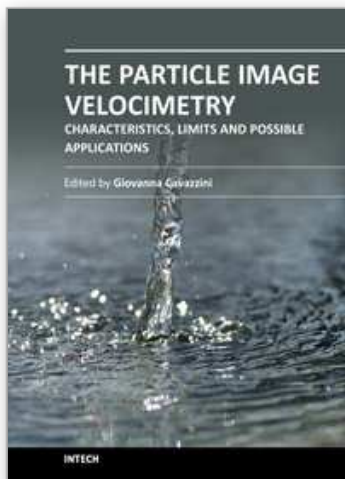
The Particle Image Velocimetry - Characteristics, Limits and Possible Applications

Edited by PhD. Giovanna Cavazzini

The Particle Image Velocimetry is undoubtedly one of the most important technique in Fluid-dynamics since it allows to obtain a direct and instantaneous visualization of the flow field in a non-intrusive way. This innovative technique spreads in a wide number of research fields, from aerodynamics to medicine, from biology to turbulence researches, from aerodynamics to combustion processes. The book is aimed at presenting the PIV technique and its wide range of possible applications so as to provide a reference for researchers who intended to exploit this innovative technique in their research fields. Several aspects and possible problems in the analysis of large- and micro-scale turbulent phenomena, two-phase flows and polymer melts, combustion processes and turbo-machinery flow fields, internal waves and river/ocean flows were considered.

How to reference

In order to correctly reference this scholarly work, feel free to copy and paste the following:

INTECH
open science | open minds